Manufacture of Energy Storage and Return Prosthetic Feet Using Selective Laser Sintering

Brian J. South

Nicholas P. Fey

Department of Mechanical Engineering,
The University of Texas at Austin,
Austin, TX 78712

Gordon Bosker
Department of Rehabilitation Medicine,
The University of Texas Health Science Center,
San Antonio, TX 78229

Richard R. Neptune[1]
Department of Mechanical Engineering,
The University of Texas at Austin,
Austin, TX 78712
e-mail: rneptune@mail.utexas.edu

Proper selection of prosthetic foot-ankle components with appropriate design characteristics is critical for successful amputee rehabilitation. Elastic energy storage and return (ESAR) feet have been developed in an effort to improve amputee gait. However, the clinical efficacy of ESAR feet has been inconsistent, which could be due to inappropriate stiffness levels prescribed for a given amputee. Although a number of studies have analyzed the effect of ESAR feet on gait performance, the relationships between the stiffness characteristics and gait performance are not well understood. A challenge to understanding these relationships is the inability of current manufacturing techniques to easily generate feet with varying stiffness levels. The objective of this study was to develop a rapid prototyping framework using selective laser sintering (SLS) for the creation of prosthetic feet that can be used as a means to quantify the influence of varying foot stiffness on transtibial amputee walking. The framework successfully duplicated the stiffness characteristics of a commercial carbon fiber ESAR foot. The feet were mechanically tested and an experimental case study was performed to verify that the locomotor characteristics of the amputee's gait were the same when walking with the carbon fiber ESAR and SLS designs. Three-dimensional ground reaction force, kinematic, and kinetic quantities were measured while the subject walked at 1.2 m/s. The SLS foot was able to replicate the mechanical loading response and locomotor patterns of the ESAR foot within ±2 standard deviations. This validated the current framework as a means to fabricate SLS-based ESAR prosthetic feet. Future work will be directed at creating feet with a range of stiffness levels to investigate appropriate prescription criteria.
[DOI: 10.1115/1.4000166]

Keywords: amputee, rapid prototyping, gait, design

1 Introduction

Recent estimates indicate that approximately 40% (623,000) of the amputees living in the United States are major lower-limb amputees, and that there will be over 1.4 million by the year 2050 [1]. Relative to nonamputees, lower-limb amputees have significant differences in a number of biomechanical quantities including reduced self-selected walking speed [2–4] and increased variability in muscle excitation patterns [5,6]. Amputees have also shown increases in gait asymmetry [5–9], intact leg loading [9], and metabolic cost [3], compared with nonamputees walking at the same speed. Thus, appropriate prosthetic component selection for amputees is critical to mitigate these detrimental effects during locomotion, and improve amputee care. Currently, patient feedback and clinical experience of the physician or prosthetist are often the primary means of component selection rather than objective biomechanical data [6,10–13]. Thus, research is needed to develop objective, quantitative selection methods for prosthetic components to improve the rehabilitation and quality of life for the growing amputee population.

An important element of prosthetic component selection is an appropriate prosthetic foot. Historically, the solid ankle cushioned heel (SACH) type design was prescribed, which aids in reducing impact loading at heel strike, but stores and releases very little elastic energy that has the potential to help improve gait. Currently, many prosthetic feet are designed and manufactured using carbon fiber (CF), a high-strength and lightweight composite, which has allowed for the successful development of energy storage and return (ESAR) feet. These feet store elastic energy during the stance phase, and release a portion of it near toe-off to aid in propulsion and leg-swing initiation [14]. A number of studies have investigated changes in gait while walking with ESAR feet (for review, see Ref. [12]), however, the relationships between foot stiffness and gait performance are not well understood [6]. Inappropriate stiffness levels could have a detrimental effect on gait performance, which may explain the inconsistent results across studies [12]. To date, no study has systematically varied prosthetic foot stiffness across a wide range of values to identify these relationships, primarily due to the high cost and difficulty in fabricating custom ESAR feet. Thus, the development of a framework utilizing rapid prototyping technology that allows for quick, cost-effective fabrication of prosthetic feet with a desired stiffness is greatly needed to facilitate such studies.

One suitable technology is selective laser sintering (SLS), a versatile and cost-effective method for rapid prototyping with reduced fabrication times, little need for human intervention, and no cost penalties for increasing design complexity [15]. In addition, SLS technology has been successfully applied to the fabrication of ankle-foot orthoses and transtibial prosthetic sockets [16–21], and is well-suited for the fabrication of prosthetic feet. The SLS process involves transforming a 3D model of a design into a series of thin, planar, cross-sectional geometries. A thin layer of powder is distributed over a part bed, and melted (sintered) together in the desired cross-sectional shape using a high-powered laser. After lowering the build space and adding another layer of powder, the next cross section is sintered to the previous layer. This sequence of adding successive sintered layers is repeated until the 3D volume is fabricated. Utilizing SLS technology would allow for rapid creation of custom prosthetic feet with precise stiffness levels that can be readily tested on amputees to investigate the relationships between foot stiffness and gait performance.

The objective of this study was to develop such a framework, based on SLS manufacturing technology to rapidly create prosthetic feet with varying stiffness characteristics that can be used in future studies as a means to quantify the influence of prosthetic foot stiffness on gait performance. To test the effectiveness of the framework, we duplicated the geometry and stiffness characteristics of a commercial ESAR foot with SLS, and used finite element analysis, mechanical testing, and experimental gait analysis to verify the SLS foot performance. The experimental gait analysis consisted of a case study with a transtibial amputee to verify that

[1]Corresponding author.

Contributed by the Bioengineering Division of ASME for publication in the JOURNAL OF BIOMECHANICAL ENGINEERING. Manuscript received May 7, 2009; final manuscript received August 18, 2009; accepted manuscript posted September 4, 2009; published online December 18, 2009. Assoc. Editor: Michael Sacks.

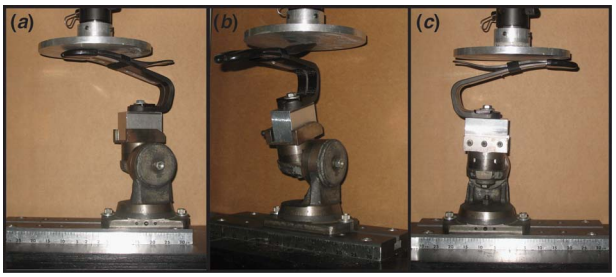

Fig. 1 Mechanical testing of the Highlander™ CF foot during the (*a*) toe-only, (*b*) heel-only, and (*c*) foot-flat conditions

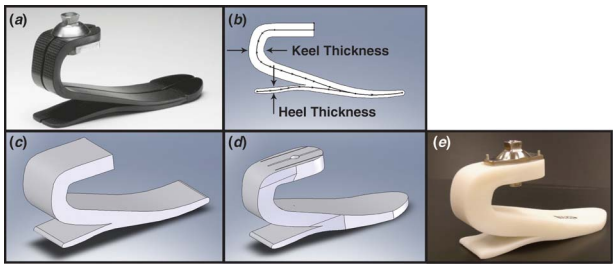

Fig. 2 Steps in deriving the CAD model for SLS fabrication from CF foot geometry: (*a*) Highlander™ (FS 3000) CF foot (Freedom Innovations, Inc.), (*b*) centerline spline curve of sagittal plane CF geometry with keel and heel thicknesses used to modify foot stiffness, (*c*) extruded geometry, (*d*) cut and trimmed CAD model ready for SLS fabrication, and (*e*) resulting prototype

the temporal, kinetic, and kinematic characteristics of the amputee's gait were the same with both the carbon fiber and SLS designs during steady-state walking.

2 Methods

The primary elements of the SLS framework included: (1) mechanically testing the commercial CF foot to obtain target stiffness data, (2) using computer-aided design (CAD) software to create a three-dimensional surface model derived from the CF foot geometry, which could be easily modified to match the desired stiffness value, (3) performing an engineering analysis using finite element methods (FEM) to assess the structural integrity of the SLS foot during normal loading conditions, (4) fabricating the SLS prototype, and (5) mechanically testing the SLS foot to verify the stiffness characteristics. The performance of the foot was validated with a case study of a single traumatic transtibial amputee. Each component of the SLS framework is described below in detail.

2.1 Testing the Carbon Fiber Foot. The ESAR foot replicated in this study was the Highlander™ foot (Freedom Innovations, Inc., Irvine, CA) made of carbon fiber with continuous sweep geometry and easily scalable geometric dimensions. The Highlander™ CF foot was mechanically tested using an Applied Test Systems (Butler, PA) universal testing machine (Model 1620) equipped with a uniaxial load cell (Fig. 1). The foot was attached to the base of the machine with a three degree-of-freedom vice, and loaded axially from the top using a flat aluminum plate attached below the load cell. Similar to Saunders et al. [22], the amount of deflection was measured as the foot was loaded in three configurations: toe-only contact (TO) up to 68 kg, heel-only contact (HO) up to 41 kg, and foot-flat (FF) up to 114 kg (Fig. 1). These loads were chosen as typical values observed over the gait cycle, and provided enough data points to obtain load-deflection curves. A preliminary study showed loading speeds ranging from 0.13 cm/min to 5.08 cm/min produced identical load-deflection curves. Therefore, a crosshead speed of 0.64 cm/min was chosen to ensure a quasistatic, yet timely test. The orientation for the FF condition was determined by ensuring both the toe and heel made contact with the loading plate simultaneously. TO and HO tests were performed individually [12] and were oriented as close as possible to FF while preventing any undesired portions of the foot from interfering with the section of interest (keel or heel). The orientation of the vice under each loading condition (2 deg plantarflexed and 9 deg dorsiflexed from FF for the TO and HO conditions, respectively) was recorded to ensure identical mechanical testing conditions for the SLS foot. All data were collected at 60 Hz.

2.2 Creation of SLS Foot CAD Model. The geometry of the Highlander™ CF foot was imported into SOLIDWORKS™ (Concord, MA) CAD software by reproducing the two-dimensional projection of the sagittal plane geometry as a centerline spline curve on a sketch plane. While maintaining the critical features of the CF foot (length, height, socket-pylon attachment locations, and ground points of contact), model thickness was altered at various points surrounding the spline to allow for the fabrication of a foot with the desired stiffness value. The closed sketch loop was then extruded to the proper width, and trimmed appropriately to match the overall shape of the CF foot. All dimensions other than keel and heel thickness were similar to the CF foot (Fig. 2). The split toe feature of the CF foot, primarily for turning stability, was omitted because of the sagittal plane walking conditions in the present case study [23,24].

2.3 FEM Analysis of SLS Foot CAD Model. The stiffness and structural integrity of the SLS foot was verified using FEM analyses in COSMOSWORKS™ (Concord, MA) using similar boundary and loading conditions of the CF foot. Virtual TO, HO, and FF loading conditions were created by constraining the appropriate portions of the foot model, and applying external loads. The mesh elements used were 3D parabolic tetrahedral solid elements with four corner nodes and six midside nodes per element. The mesh generator automatically adjusted the size of the elements if the local mesh was too large for a smooth transition between geometric features. The complete FEM mesh contained 14,602 elements and 23,446 nodes. The material properties for Rilsan™ D80 (Table 1) were used for the CAD models. To achieve the desired stiffness, an iterative design process was used. The

Table 1 Material properties for Rilsan™ D80

Density	Yield strength	Ultimate tensile strength	Tensile modulus	Poisson's ratio
1.04 g/cm^3	35 MPa	50 MPa	868 MPa	0.39

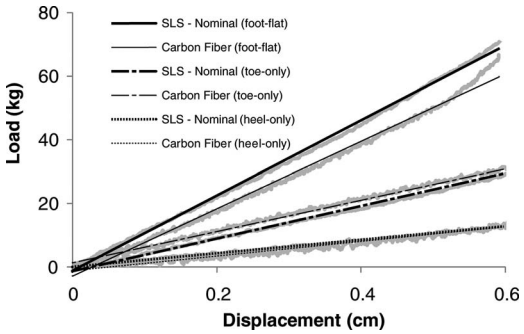

Fig. 3 Stiffness data for SLS versus CF feet in the toe-only, foot-flat, and heel-only conditions. Measurement data (light gray) was fit with a linear regression line. All data were truncated at 0.6 cm displacement for ease of comparison.

Table 2 Average (± standard deviation) spatiotemporal gait parameters for the CF. Also shown are the percent differences between the SLS and CF feet. All SLS values were within the variability of the CF foot and all differences were less than 3%.

		Residual leg		Intact leg	
		Exp. value	Deviation from CF (%)	Exp. value	Deviation from CF (%)
Step length (m)	CF	0.76 ± 0.021	–	0.71 ± 0.018	–
	SLS	0.76 ± 0.018	0.39	0.70 ± 0.017	−1.13
Step time (s)	CF	0.62 ± 0.020	–	0.63 ± 0.020	–
	SLS	0.63 ± 0.020	1.61	0.62 ± 0.020	−1.59
Stance time (s)	CF	0.79 ± 0.020	–	0.80 ± 0.020	–
	SLS	0.77 ± 0.020	−2.53	0.79 ± 0.020	−1.25
Cycle time (s)	CF	1.26 ± 0.020	–	1.26 ± 0.020	–
	SLS	1.25 ± 0.030	−0.79	1.25 ± 0.030	−0.79
Steps/min	CF	96.2 ± 2.29	–	94.7 ± 2.46	–
	SLS	95.7 ± 3.25	−0.57	96.3 ± 2.74	1.69

thicknesses of the keel and heel sections were adjusted independently until the required deformation of the model (heel and keel) during the loading conditions was reached. Locations of stress concentration were noted, and material was added to ensure the maximum stress did not exceed the yield strength of the material.

2.4 Fabrication and Testing of SLS Feet. Once the desired stiffness was achieved, the CAD model was exported in stereolithography (STL) file format, and used to fabricate the SLS foot out of Rilsan™ D80 using a Vanguard HiQ Sinterstation (3DSystems, Valencia, CA). Rilsan™ D80 (Nylon 11, Arkema, France,) was used to make the SLS feet, due to its desirable material properties for making prosthetic components [20]. The foot was oriented in the build volume, such that each successive layer of powder was parallel to the sagittal plane of the foot to avoid any potential weaknesses resulting from layer delamination. The automated SLS build process required 3 h of warm up, 8 h of build time, and 4 h of cool down time, resulting in a total build time of 15 h.

Mechanical testing of the SLS foot included identical orientations and loading conditions of the CF foot. In addition, high load tests were performed on the SLS foot to ensure that the foot would not undergo permanent deformation or fracture under normal walking conditions. The SLS foot was placed under a high load of 272 kg (i.e., greater than three times the expected bodyweight) in the foot flat condition. Permanent deformation was assessed through visual observation and external dimension measurement.

2.5 Experimental Data Collection. To assess the biomechanical response of the foot, a case study was performed with a

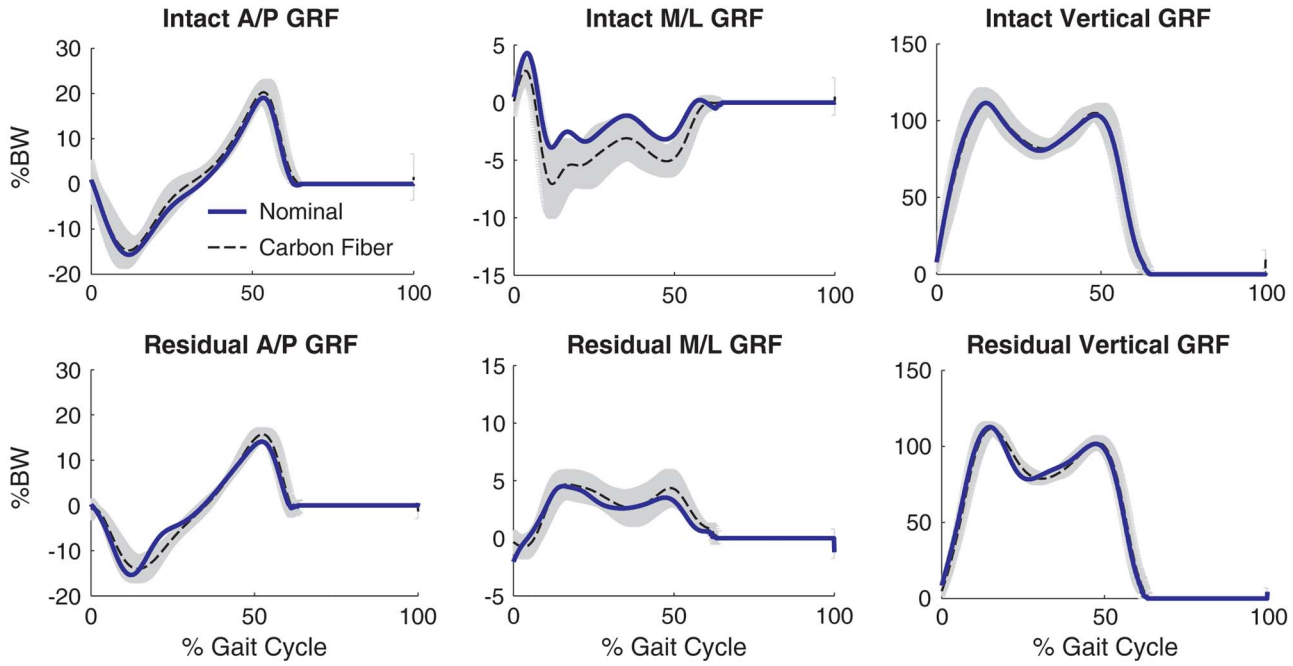

Fig. 4 Comparison of the intact and residual leg ground reaction forces between the SLS and CF (±2 standard deviations, shaded area) feet. The mean of the SLS foot was nearly always within two standard deviations, shaded area of the CF foot mean.

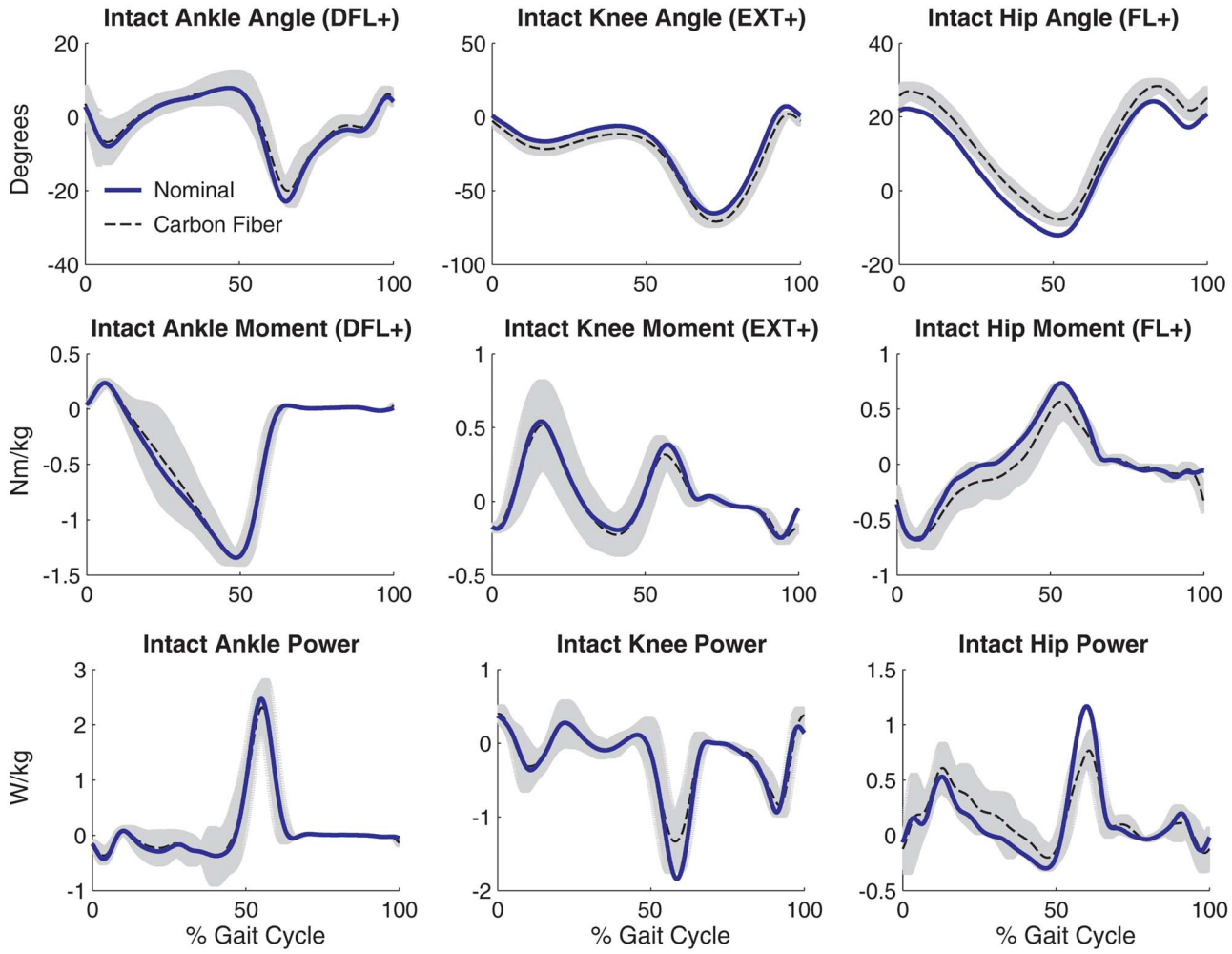

Fig. 5 Comparison of the intact leg joint angles, moments, and powers between the SLS and CF (±2 standard deviations, shaded area) feet. The mean of the SLS foot was nearly always within two standard deviations of the CF foot mean.

45-year-old traumatic, transtibial, unilateral amputee (1.87 m, 78.5 kg) who was a proficient walker. The subject was in good physical condition with no musculoskeletal disorders or pain, and had been an amputee for over 16 years. A licensed prosthetist with 30 years of experience was present during data collection, and ensured proper alignment of the CF and SLS feet. Mass (80 g) was added to the CF foot near the center of mass to ensure both feet had similar inertial properties. The subject provided informed consent approved by The University of Texas and the South Texas VA Medical Center.

Both the CF and SLS feet were tested during repeated walking trials. For each trial, the subject walked along a 10-m walkway containing four embedded and concealed force plates (46.4 $\times 50.8$ cm^2; Advanced Mechanical Technology Inc., Watertown, MA). Infrared timing gates were used to ensure the subject met the desired walking speed of 1.2 ± 0.06 m/s, which was a speed near the subject's preferred walking speed. A verbal cue was given to begin walking, and verbal feedback on walking speed was provided after each trial indicating whether the speed requirement was met. The trials were repeated until ten force plate hits were recorded for each leg.

Kinematic data were collected at 120 Hz, and ground reaction force (GRF) data were collected at 1200 Hz using Vicon Workstation (Version 5.1, Oxford Metrics, Oxford, UK). Reflective markers (14 mm in diameter) were placed on the C-7 vertebrae and bilaterally on the acromion, iliac crest, posterior superior iliac spine, anterior superior iliac spine, greater trochanter, lateral and medial femoral condyles, lateral and medial malleoli, heel, dorsal foot, and the first, second, and fifth metatarsal head. Marker clusters were also placed bilaterally on the shank and thigh. Marker locations on the foot of the residual leg were placed such that the markers were symmetric with the intact leg.

2.6 Experimental Data Analysis. Kinetic and kinematic data were analyzed using VISUAL3D (C-Motion, Inc., Germantown, MD). A low-pass fourth order Butterworth filter with a cutoff frequency of 6 Hz was applied to the kinematic data, while GRF data were low-pass filtered at 20 Hz. Joint angles, moments, and powers were determined using standard inverse-dynamics techniques in VISUAL3D. Residual leg inertial properties were based on that of Mattes et al. [25]. GRF and kinetic data were normalized to the subject's bodyweight and body mass, respectively, and all data were normalized to the gait cycle.

Bilateral spatiotemporal gait characteristics were compared between the CF and SLS feet for the intact and residual legs, including step length, steps per minute, and step, stance, and cycle times. Both the intact and residual legs were examined to assess whether the SLS foot induced compensatory changes in the intact leg. Joint angles, moments, and powers were evaluated at the hip, knee, and ankle for both legs by computing the average absolute difference between quantities after normalization to the gait cycle. GRFs were also compared for both legs across feet conditions. All GRF, kinetic, kinematic, and spatiotemporal parameters were averaged across trials for each foot.

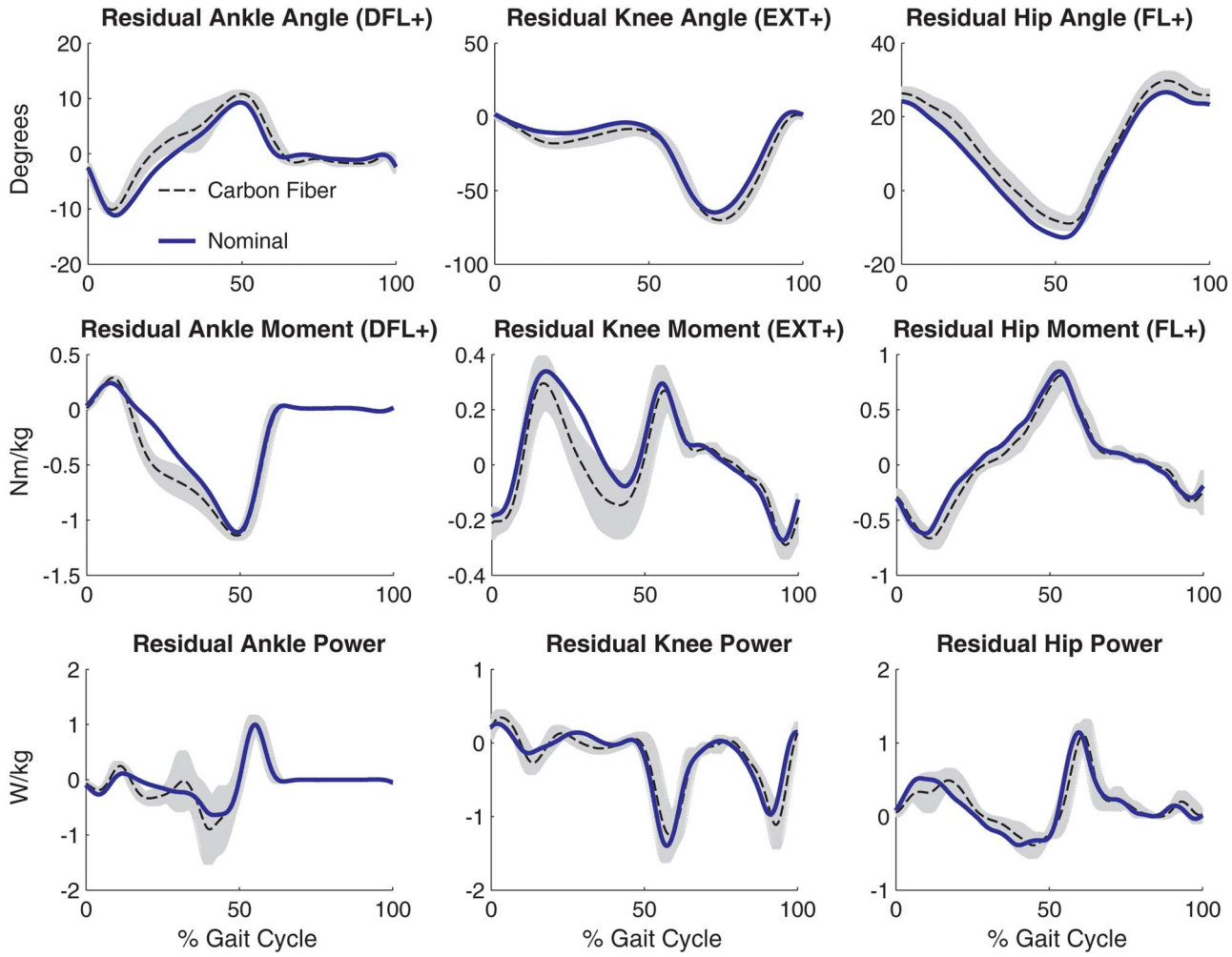

Fig. 6 Comparison of the residual leg joint angles, moments and powers between the SLS and CF (±2 standard deviations, shaded area) feet. The mean of the SLS foot was nearly always within two standard deviations of the CF foot mean.

3 Results

The SLS framework produced a prosthetic foot with similar stiffness characteristics as the CF foot (Fig. 3), and did not fail or exhibit any permanent deformation during the high load testing. The similar stiffness characteristics resulted in spatiotemporal, kinetic, and kinematic gait characteristics that were nearly identical when the subject walked with the CF and SLS feet. All spatiotemporal gait parameters for the SLS foot were within ~2.5% of the CF foot (Table 2) for both the residual and intact legs. Both the intact and residual leg GRFs were nearly identical, with the SLS foot nearly always within two standard deviations of the CF foot (Fig. 4). The only exception was the intact leg medial/lateral GRF, which showed a slight offset in magnitude, although the pattern and temporal phasing were the same (Fig. 4). The intact and residual leg joint angles, moments, and powers, while wearing the SLS foot, were all similar to the CF foot and almost always within two standard deviations of the CF foot (Figs. 5 and 6). The average joint angle deviation between the CF and SLS feet for the intact and residual legs was 3.14 deg and 3.53 deg, respectively. The average deviations in the joint moments were 0.064 N m/kg and 0.046 N m/kg, while the average deviations in the joint powers were 0.090 W/kg and 0.071 W/kg, respectively.

4 Discussion

The objective of this study was to develop a framework based on SLS manufacturing technology to rapidly design and fabricate prosthetic feet with custom stiffness levels for detailed studies designed to understand the relationships between foot stiffness and gait performance in transtibial amputee walking. This framework successfully reproduced the CF foot's stiffness characteristics. Mechanical testing of the foot verified that the proposed framework produced a SLS foot that performed similarly to the CF foot. In addition, the high load testing showed the SLS foot does not fail under high loads nor show any permanent deformation. The spatiotemporal, kinematic, and kinetic gait characteristics of the CF foot were nearly identical when the subject walked with the SLS foot. Some minor differences were noted between the SLS and CF feet in the residual leg ankle and knee moments during midstance. However, additional modifications of the foot design such as refinements of the keel stiffness could further reduce these differences between feet.

One of the more time consuming aspects of the framework was recreating the geometry of the Highlander™ CF foot by reproducing the two-dimensional projection of the sagittal plane geometry, and extruding that geometry to the proper width. The geometry was then trimmed to match the overall shape of the CF foot, and additional design features were incorporated (e.g., socket-pylon attachment locations). This step could be automated using various imaging techniques. For example, we have previously used a laser scan of the residual limb to generate custom prosthetic socket shapes [17,18] and CT scans to import the geometry of a commercial ankle-foot orthosis [20]. These techniques could be easily adapted to automate the generation of the initial foot geometry.

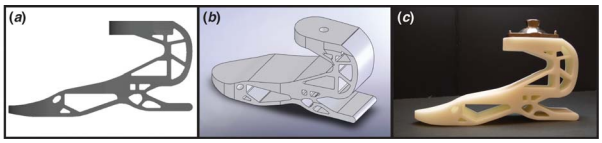

Fig. 7 The application of topology optimization techniques to develop novel prosthetic foot designs for manufacture using SLS technology. The example above sought to replicate the stiffness characteristics of the CF foot while minimizing the material used: (*a*) sagittal plane optimization solution, (*b*) corresponding 3D CAD model, and (*c*) resulting SLS prototype.

One potential limitation of the current framework is the lack of information regarding the response of SLS feet to impact loading. Although these types of loading responses are not of primary concern for steady-state walking conditions, resistance to dynamic loading could be of greater importance for active walkers. Similarly, the long-term fatigue characteristics of the SLS material were not assessed. Thus, future work should be directed towards investigating the impact response and fatigue properties of the SLS feet. In addition, we used a quasistatic method to measure the stiffness using a uniaxial load cell. Since we tested both the CF and SLS foot using an identical protocol, this approach was deemed justified. However, a more complete characterization of the stiffness properties may be possible using a dynamic gait simulator (e.g., see Ref. [26]).

The versatility of the SLS manufacturing process allows for easy scaling or the inclusion of additional features that would otherwise be difficult or impossible to incorporate into the design. Techniques such as topology optimization [27,28] were previously used to create unique features in SLS fabricated sockets [28], and could be used to optimize design features and produce novel foot designs. For example, we used topology optimization techniques to design a foot that maintained the overall foot stiffness characteristics of the CF foot while minimizing the amount of SLS material used (Fig. 7).

Overall, the SLS framework produced prosthetic feet with mechanical properties that were similar to the desired CF properties, and we believe that this could be used to generate feet with a carefully controlled array of stiffness levels and geometries. Experienced amputees often have an incredible ability to adapt and maintain kinematic similarity despite significant changes to components and alignment. Thus, SLS could be used to create feet with a wide range of stiffness levels to identify neuromotor and biomechanical adaptations that occur and understand the relationships between foot stiffness and gait performance. Once these relationships are understood, the presented SLS framework could be used to fabricate customized, subject-specific prosthetic feet with appropriate stiffness levels to improve the rehabilitation and quality of life for the growing amputee population.

Acknowledgment

The authors would like to thank Gail Walden and Rosie Trevino for help with the data collection, Dr. Eric Taleff for his help with the stiffness measurements, and Dr. Glenn Klute for his insightful comments on the manuscript. This project was supported by the National Science Foundation under Grant No. 0346514.

References

[1] Ziegler-Graham, K., MacKenzie, E. J., Ephraim, P. L., Travison, T. G., and Brookmeyer, R., 2008, "Estimating the Prevalence of Limb Loss in the United States: 2005 to 2050," Arch. Phys. Med. Rehabil., **89**(3), pp. 422–429.

[2] Robinson, J. L., Smidt, G. L., and Arora, J. S., 1977, "Accelerographic, Temporal, and Distance Gait Factors in Below-Knee Amputees," Phys. Ther., **57**(8), pp. 898–904.

[3] Czerniecki, J., and Gitter, A., 1996, "Gait Analysis in the Amputee: Has it Helped the Amputee or Contributed to the Development of Improved Prosthetic Components," Gait and Posture, **4**, pp. 258–268.

[4] Perry, J., Boyd, L. A., Rao, S. S., and Mulroy, S. J., 1997, "Prosthetic Weight Acceptance Mechanics in Transtibial Amputees Wearing the Single Axis, Seattle Lite, and Flex Foot," IEEE Trans. Rehabil. Eng., **5**(4), pp. 283–289.

[5] Winter, D. A., and Sienko, S. E., 1988, "Biomechanics of Below-Knee Amputee Gait," J. Biomech., **21**(5), pp. 361–367.

[6] Klute, G. K., Kallfelz, C. F., and Czerniecki, J. M., 2001, "Mechanical Properties of Prosthetic Limbs: Adapting to the Patient," J. Rehabil. Res. Dev., **38**(3), pp. 299–307.

[7] Breakey, J., 1976, "Gait of Unilateral Below-Knee Amputees," Orthot. Prosthet., **30**(3), pp. 17–24.

[8] Hermodsson, Y., Ekdahl, C., Persson, B. M., and Roxendal, G., 1994, "Gait in Male Trans-Tibial Amputees: A Comparative Study With Healthy Subjects in Relation to Walking Speed," Prosthet. Orthot Int., **18**(2), pp. 68–77.

[9] Royer, T. D., and Wasilewski, C. A., 2006, "Hip and Knee Frontal Plane Moments in Persons with Unilateral, Trans-Tibial Amputation," Gait and Posture, **23**(3), pp. 303–306.

[10] Macfarlane, P. A., Nielsen, D. H., Shurr, D., and Meier, K., 1991, "Perception of Walking Difficulty by Below-Knee Amputees Using a Conventional Foot Versus the Flex-Foot," J. Prosthet. Orthot., **3**(3), pp. 114–119.

[11] Postema, K., Hermens, H. J., de Vries, J., Koopman, H. F., and Eisma, W. H., 1997, "Energy Storage and Release of Prosthetic Feet. Part 2: Subjective Ratings of 2 Energy Storing and 2 Conventional Feet, User Choice of Foot and Deciding Factor," Prosthet. Orthot. Int., **21**(1), pp. 28–34.

[12] Hafner, B. J., Sanders, J. E., Czerniecki, J., and Fergason, J., 2002, "Energy Storage and Return Prostheses: Does Patient Perception Correlate With Biomechanical Analysis?" Clin. Biomech. (Bristol, Avon), **17**(5), pp. 325–344.

[13] Fridman, A., Ona, I., and Isakov, E., 2003, "The Influence of Prosthetic Foot Alignment on Trans-Tibial Amputee Gait," Prosthet. Orthot Int., **27**(1), pp. 17–22.

[14] Hafner, B. J., Sanders, J. E., Czerniecki, J. M., and Fergason, J., 2002, "Transtibial Energy-Storage-and-Return Prosthetic Devices: A Review of Energy Concepts and a Proposed Nomenclature," J. Rehabil. Res. Dev., **39**(1), pp. 1–11.

[15] Beaman, J. J., 1997, *Solid Freeform Fabrication: A New Direction in Manufacturing: With Research and Applications in Thermal Laser Processing*, Kluwer, Dordrecht.

[16] Faustini, M. C., Crawford, R. H., Neptune, R. R., Rogers, W. E., and Bosker, G., 2005, "Design and Analysis of Orthogonally Compliant Features for Local Contact Pressure Relief in Transtibial Prostheses," J. Biomech. Eng., **127**(6), pp. 946–951.

[17] Faustini, M. C., Neptune, R. R., and Crawford, R. H., 2006, "The Quasi-Static Response of Compliant Prosthetic Sockets for Transtibial Amputees Using Finite Element Methods," Med. Eng. Phys., **28**(2), pp. 114–121.

[18] Faustini, M. C., Neptune, R. R., Crawford, R. H., Rogers, W. E., and Bosker, G., 2006, "An Experimental and Theoretical Framework for Manufacturing Prosthetic Sockets for Transtibial Amputees," IEEE Trans. Neural Syst. Rehabil. Eng., **14**(3), pp. 304–310.

[19] Rogers, B., Bosker, G. W., Crawford, R. H., Faustini, M. C., Neptune, R. R., Walden, G., and Gitter, A. J., 2007, "Advanced Trans-Tibial Socket Fabrication Using Selective Laser Sintering," Prosthet. Orthot Int., **31**(1), pp. 88–100.

[20] Faustini, M. C., Neptune, R. R., Crawford, R. H., and Stanhope, S. J., 2008, "Manufacture of Passive Dynamic Ankle-Foot Orthoses Using Selective Laser Sintering," IEEE Trans. Biomed. Eng., **55**(2), pp. 784–790.

[21] Rogers, B., Bosker, G. W., Faustini, M. C., Walden, G., Neptune, R. R., and Crawford, R. H., 2008, "Case Report: Variably Compliant Transtibial Prosthetic Socket Fabricated Using Solid Freeform Fabrication," J. Prosthet. Orthot., **20**(1), pp. 1–7.

[22] Saunders, M. M., Schwentker, E. P., Kay, D. B., Bennett, G., Jacobs, C. R., Verstraete, M. C., and Njus, G. O., 2003, "Finite Element Analysis as a Tool for Parametric Prosthetic Foot Design and Evaluation. Technique Development in the Solid Ankle Cushioned Heel (SACH) Foot," Comput. Methods Biomech. Biomed. Eng., **6**(1), pp. 75–87.

[23] van Jaarsveld, H. W., Grootenboer, H. J., de Vries, J., and Koopman, H. F., 1990, "Stiffness and Hysteresis Properties of Some Prosthetic Feet," Prosthet. Orthot Int., **14**(3), pp. 117–124.

[24] Underwood, H. A., Tokuno, C. D., and Eng, J. J., 2004, "A Comparison of Two Prosthetic Feet on the Multi-Joint and Multi-Plane Kinetic Gait Compensations in Individuals With a Unilateral Trans-Tibial Amputation," Clin. Biomech. (Bristol, Avon), **19**(6), pp. 609–616.

[25] Mattes, S. J., Martin, P. E., and Royer, T. D., 2000, "Walking Symmetry and Energy Cost in Persons With Unilateral Transtibial Amputations: Matching Prosthetic and Intact Limb Inertial Properties," Arch. Phys. Med. Rehabil., **81**(5), pp. 561–568.

[26] Aubin, P. M., Cowley, M. S., and Ledoux, W. R., 2008, "Gait Simulation Via a 6-DOF Parallel Robot With Iterative Learning Control," IEEE Trans. Biomed. Eng., **55**(3), pp. 1237–1240.

[27] Svanberg, K., 1987, "The Method of Moving Asymptotes—A New Method for Structural Optimization," Int. J. Numer. Methods Eng., **24**(2), pp. 359–373.

[28] Sigmund, O., 2001, "A 99 Line Topology Optimization Code Written in MATLAB," Struct. Multidiscip. Optim., **21**(2), pp. 120–127.